agronomy

MDPI

Article

Application of Biosynthesized Silver Nanoparticles from Oak Fruit Exudates against *Pectobacterium carotovorum* subsp. *carotovorum* Causing Postharvest Soft Rot Disease in Vegetables

Meysam Soltani Nejad [1,*], Neda Samandari Najafabadi [2], Sonia Aghighi [3,*], Meisam Zargar [4,*], Gani Stybayev [5], Aliya Baitelenova [5] and Gulden Kipshakbayeva [5]

[1] Department of Plant Protection, Faculty of Agriculture, Shahid Bahonar University of Kerman, Kerman 76169-14111, Iran
[2] Department of Plant Protection, Faculty of Agriculture, Ferdowsi University of Mashhad, Mashhad 91779-48978, Iran; samandarinajafabadi.neda@mail.um.ac.ir
[3] Research and Technology Institute of Plant Production (RTIPP), Shahid Bahonar University of Kerman, Kerman 76169-14111, Iran
[4] Department of Agrobiotechnology, Institute of Agriculture, RUDN University, 117198 Moscow, Russia
[5] Department of Plant Production, Faculty of Agronomy, S. Seifullin Kazakh Agrotechnical University, Astana 010000, Kazakhstan; g.stybaev@kazatu.edu.kz (G.S.); a.baitelenov@kazatu.edu.kz (A.B.); g.kipshakbaeva@kazatu.edu.kz (G.K.)
* Correspondence: meysamsoltaninejad@agr.uk.ac.ir (M.S.N.); aghighis@uk.ac.ir (S.A.); zargar_m@pfur.ru (M.Z.)

check for updates

Citation: Soltani Nejad, M.; Samandari Najafabadi, N.; Aghighi, S.; Zargar, M.; Stybayev, G.; Baitelenova, A.; Kipshakbayeva, G. Application of Biosynthesized Silver Nanoparticles from Oak Fruit Exudates against *Pectobacterium carotovorum* subsp. *carotovorum* Causing Postharvest Soft Rot Disease in Vegetables. *Agronomy* **2023**, *13*, 1624. https://doi.org/10.3390/agronomy13061624

Academic Editor: Jianye Chen

Received: 13 May 2023
Revised: 9 June 2023
Accepted: 15 June 2023
Published: 16 June 2023

Copyright: © 2023 by the authors. Licensee MDPI, Basel, Switzerland. This article is an open access article distributed under the terms and conditions of the Creative Commons Attribution (CC BY) license (https://creativecommons.org/licenses/by/4.0/).

Abstract: The main goal of our study was to determine whether biosynthesized silver nanoparticles (SNPs) could be used as a novel antibacterial material in order to control soft rot in vegetables. Exudates from oak fruit were used in the green synthesis of SNPs. Postharvest soft rot disease in vegetables has resulted in significant crop losses all over the globe. Because managing *Pectobacterium carotovorum* subsp. *carotovorum* (*Pcc*), the causal agent of soft rot disease, is difficult due to its wide host range, developing innovative disease-management methods that do not involve the use of hazardous chemicals is a top priority for maintaining sustainable agriculture. The current research has found that silver nanoparticles (SNPs) have a detrimental effect on the progression of *Pcc* and soft rot disease in in vitro conditions. At SNPs' sub-MIC, the greatest levels of inhibition against tissue maceration were 22, 19.8, 21.5, and 18.5 percent in potato, zucchini, carrot, and eggplant, respectively. SNP treatment of tubers and fruits had a noteworthy suppressive impact on soft rot disease symptoms as compared to controls. SNPs may be able to replace chemical pesticides in the management and prevention of soft rot disease in vegetables in postharvest settings, according to this study.

Keywords: postharvest soft rot; nanosilver; vegetables; biosynthesis; *Quercus brantii* L.; *Pectobacterium carotovorum* subsp. *carotovorum*

1. Introduction

Nanotechnology advancements over the last decades have had tremendous impacts on various aspects of science. Nanotechnology has emerged as a vital topic of contemporary research with wide-ranging implications in a variety of fields [1,2]. Nano-researchers are fascinated by the biosynthesis of silver nanoparticles (SNPs or AgNPs), using diverse biological approaches [3]. Nanoparticles (NPs) contain unique biological features such as antibacterial [4], magnetic [5], and catalytic abilities [6], resulting in an increasing use of nanomaterials in research applications such as the production of novel insecticides to combat plant diseases [7], nanomedicine [8], electrochemical biosensors [9], nanocomposite, and food safety [10]. Furthermore, nanobiotechnology has applications in all fields of food science, such as agriculture; prospective uses include agrochemical delivery, novel insecticides, genetic engineering, sensors of monitor soil conditions, postharvest loss reduction, food processing, and due to their effects on the environment and human health, they should be consumed with caution. [11,12]. Nanoparticles (NPs) can be synthesized via a variety of techniques, including physical, chemical, and biological approaches [13]. New green techniques for the synthesis of metal nanoparticles (NPs) are being developed by utilizing plant-based materials and microorganisms such as bacteria and fungi in order to retrieve high quantities of low-cost, and biocompatible materials [14–16]. Moreover, the green-synthesized SNPs using plant-based derivatives can be adjusted and controlled to attain the desired shape and size. These AgNPs, biosynthesized from naturally derived materials, are not only safe, economical, and eco-friendly, but also simple and convenient, which is encouraging researchers to explore greener routes and viable options, utilizing different parts of plants such as flowers, stems, petal, leaves, and carbohydrates such as chitosan to meet these demands [17].Green synthesis technology and protocols, through the application of plant materials and silver nanoparticles, offer a promising avenue for the production of sustainable products.

Many plant species have been utilized to synthesize SNPs with antibacterial action in different sizes of nanoparticles. SNPs were produced from aqueous leaf extracts of *Ctenolepis garcini* by Narayanan et al. [18] and the SNPs have shown antibacterial and antioxidant activity. In specific circumstances, Jalab et al. [19] employed *Acacia cyanophylla* extract as a reducing agent to prepare stable SNPs, which had a strong antibacterial activity.

The application of nanomaterials in plant protection—specially, plant pathology—is developing. Potato (*Solanum tuberosum*) is an important crop and a key resource for meeting the demands of the world's growing population, ranking fourth in the world's most valued tuber crops [20]. Soft rot is one of the most common bacterial postharvest diseases in vegetables. *Pectobacterium carotovorum* is a pectolytic bacterium belonging to the *Enterobacteriaceae* family that causes tissue soft rot [21]. Soft rot disease, produced by *Pectobacterium* species on potatoes, zucchini, carrots, and eggplant, may damage the storage of tubers and fruit as well as the quality of these products. *Pectobacterium carotovorum* subsp. *carotovorum* (*Pcc*) has the broadest worldwide host range of all the *Pectobacterium* spp. that infect potatoes [22,23]. This subspecies, which is a key agent of tuber rot in bulk storage conditions in Iran, causes the deterioration of potato tubers [24,25]. Moreover, *Pectobacterium carotovorum* is one of the most dangerous potato diseases, increasing the cost in potato storage across the globe by generating bacterial contamination both in the field and after harvesting [26]. Symptoms in zucchini (*Cucurbita pepo*) fruit initially appear as wet rot on the surface of the infected tissues and water soaking in the infected fruit. Subsequently, rot symptoms expand and progress to brown rot in the fruit, caused by *Pcc* [27]. Carrots (*Daucus carota* L.) are very susceptible to soft rot bacterial infection. The bacterium, *Pcc*, causes soft rot. The symptoms of a major spread appear as a soft rot and the watery, slimy decay of the taproot [28]. According to research, only *Pcc* has been reported as causing fruit rot in eggplant (*Solanum melongena*) [29].

Control of industrial crop disease has become more common in recent years, in order to increase environmental safety and economic efficiency, and novel techniques to battle phytopathogens, using innovative approaches, are of particular importance [30].

Farmers use a considerable number of toxic pesticides to manage soft rot disease each year, which not only adds to expenses in the short-term but also has long-term consequences for human health [31,32]. We undertook the production of SNPs from oak (*Quercus brantii* L.) fruit exudates, which have been used in traditional Iranian medicine. This plant is traditionally used to treat human health problems such as gastropathy, acute diarrheal inflammation, burns and cuts, and cancers.

In the present study, we have investigated the MIC and sub-MIC concentrations of SNPs as a novel antibacterial agent to reduce the pathogenic activity of bacterial soft rot in vegetables, with the goal of more environmentally friendly production at a lower cost. Within semi-practical storage conditions, the curative effects of SNPs on soft rot were explored.

2. Materials and Methods

2.1. Reagents and Source of the Pathogen

Merck Company, Germany, provided silver nitrate ($AgNO_3$) and nutritional agar (NA). The Iranian Research Institute of Plant Protection (IRIPP) provided a virulent strain of *Pcc* (strain 84), which was cultured on the NA. Fresh vegetables, sourced from Baft vegetable farms, Kerman Province, Iran, were used in this study, including potato, zucchini, eggplant, and carrot. For this purpose, healthy vegetables with consistent sizes and no mechanical damage were chosen.

2.2. Preparation of Oak Fruits Exudates

Dry fruit were employed to make cork oak (*Quercus brantii* L.) fruit exudates. The nut section was disinfected with 75 percent ethanol after the fruit wall (pericarp) was removed, then with double-sterilized water three times. After three days of incubation at room temperature in darkness, ten grams of clean small parts were inserted in small test tubes in 150 mL deionized water, and the segments were withdrawn from the soaking media. (Figure 1a and exudates after 24 h, Figure 1b) Whatman No. 1 filter paper was used to filter the supernatant exudate [33]. The exudate was kept at 4 °C until it was needed. During the studies, the pH of the exudates was 5.5.

Figure 1. Fruits and segments of cork oak (**a**,**b**) oak fruits exudates after 24 h.

2.3. Green Synthesis of Silver Nanoparticles

Aqueous silver nitrate ($AgNO_3$) (10 mL of 10^{-3} M) was applied to 150 mL of exudates for biogenesis of silver nanoparticles (SNPs) in order to decrease Ag^+ to Ag^0. The sample was held at room temperature in a stationary position for around 120 min for the bioreduction procedure; however, no agitation or shaking was incorporated. About 120 min later, the outcomes of the mixtures were analyzed for bioreduction of Ag^+ and biosynthesis of AgNPs. To assess and evaluate color development in treated samples, control samples (exudates without silver nitrate) were employed (mixtures of exudates plus 0.01 M $AgNO_3$ solution). Exudates are also utilized as blanks in biosynthesized SNPs instrumental studies [34]. UV-visible (UV-vis) spectrophotometer analysis was used to assess the production of SNPs from cork oak fruit exudates. Transmission electron microscopy (TEM), atomic force microscopy (AFM), and X-ray diffraction spectroscopy were used to analyze the synthesized SNPs (XRD).

2.4. UV-Vis Spectroscopy Analysis of SNPs

The generation of SNPs from cork oak fruit exudates was validated three times at room temperature, using a UV-visible spectrophotometer (Epoch2TC, Highland Park, IL, USA). At room temperature, the absorption wavelength was measured between 300 and 550 nm after 30, 60, and 120 min of reaction. Color shifts from colorless $AgNO_3$ to a variety of deep brown hues were considered to indicate likely Ag^+ to Ag^0 conversion; however, UV-vis spectroscopy was employed to confirm this preliminary assumption [35].

2.5. Physicochemical Properties of SNPs (TEM, AFM, XRD, DLS and FTIR)

The morphological characterization and size of SNPs were determined using a transmission electron microscope (TEM), specifically, using a Carl ZEISS Transmission Electron Microscope (Germany). Atomic force microscopy (AFM) was used to examine the surfaces of SNPs [36].

Using a high-resolution X-ray diffraction (XRD) method, the production of compounds, quality, phase identification, and characterization of crystalline metallic SNPs were investigated. The scanning was carried out in the two-dimensional range of 30° to 80°.

The sample of SNPs was employed for research of Fourier transform infrared spectroscopy (FTIR) by centrifuging the phytosynthesized SNP solution at 10,000 rpm for five minutes. Using the KBr pellet method and a Thermo Electron Nicolet Avatar 370 DTGS FTIR spectrophotometer, the powder of the SNP solution used for FTIR analysis was recorded in the region of 4000 to 400 cm^{-1}.

The newly biosynthesized SNPs were determined using the dynamic light-scattering (DLS) technology, which was developed by Cordouan Technologies in France. Temperature was 25 °C, the laser power transmission was 50%, DTC position was up, wavelength was 657.00 nm, and all measurements were done in triplicates.

The average value of the zeta potential (z-average) and the polydispersity index are two parameters that may be obtained using the DLS approach (PDI). The z-average has been calculated.

2.6. Antibacterial Assays

Fresh *Pcc* culture in Luria–Bertani medium (LB) was applied to the surface of nutrient agar (NA) (Quelab, Montreal, Canada, 22 g/L) with 100 µL of *Pcc* suspension of 1×10^8 CFU/mL. After 45 min, 20 micro liters of biosynthesized SNPs were placed onto sterile blank paper discs at a final concentration of 50 µg/mL (6 mm). The widths of bacterial growth inhibition zones surrounding the discs were determined after plates were incubated at 28 °C for 24 h. Streptomycin was used as a positive control, while exudates from oak cork were used as a negative control. The diameter of growth inhibition zones was measured after the incubation period. The trials were carried out three times.

2.7. Determination of Minimum Inhibitory Concentration (MIC) and Minimum Bactericidal Concentration (MBC)

The *Pcc* was cultivated in LB medium overnight at 28 ± 1 °C to assess the MIC and MBC using the micro-dilution technique described by Akhlaghi et al. [37]. To achieve 500 µg/mL of SNPs in the first well of each row in 96-well microplates, 100 µL of SNPs were put to 100 µL of Mueller Hinton broth medium. SNPs were then serially 2× diluted in 96-well microplates with concentrations ranging from 500 to 0. 48 µg/mL in a total volume of 200 µL. After that, each well was infected with ten microliters of overnight bacterial culture (100 CFU/mL). At 28 ± 1 °C, the plate was incubated for one day. MIC was calculated as the lowest concentration of SNPs at which there was no discernible growth (increase in turbidity). To measure MBC, ten microliters of each bacterial culture from the wells with greater concentrations than the MIC were cultivated on the NA for 24 h at 28 °C. On the NA medium, MBC was defined as the lowest concentration with no bacterial growth. All of the tests were repeated three times.

2.8. Growth Studies of Pcc

SNPs with selected sub-inhibitory levels were added to LB broth medium in 96-well plates. At that moment, a *Pcc* subculture produced in fluid LB was balanced to 1×10^6 CFU/mL and swapped to the wells, with LB medium and exudate serving as the blank and solvent controls, respectively. All plates were held at room temperature with 125 rpm shaking, and density at 600 nm was measured using a microplate reader at five-hour intervals up to 35 h. The experiment was repeated three times with five duplicates each time.

2.9. In Vivo Evaluation of the SNPs against Soft Rot Disease on Potato Tubers, Carrot Roots and Fruits of Zucchini and Eggplant

Fresh vegetables were purchased from an Iranian vegetable market in Kerman. This study focused on healthy potato tubers, carrot roots, and zucchini and eggplant fruit that were consistent in size and free of mechanical damage. The soft rot pathogenicity experiment was used to investigate the role of SNPs in reducing disease symptoms on vegetable tissue. The vegetables were washed three times with distilled water before being disinfected with 5% sodium hypochlorite and dried. Bacterial cultures were centrifuged overnight and suspended in double sterile distilled water with a turbidity of 0.3 at 600 nm (1×10^8 CFU/mL). After adding SNPs sub-MIC concentration diluted in Tween 20 (one percent) to the solution, 200 µL of suspension was injected into the 1 mm depth of vegetable tissues using insulin needles. Infected tissues were stored in humidified plastic containers at 26 degrees Celsius. The tubers' initial weight (IW) was recorded, then the decaying tissue was scooped and removed from the tubers and weighed (DW) after 48 h. Formula 1 was used to assess the proportion of symptomatic tissue: (1) Decay (%) = (DW/IW) $\times$ 100 [23]. The findings were compared with controls (tubers and fruit inoculated with *Pcc* suspensions only).

2.10. Investigation on the Curative Activity of SNPs against Pcc In Vivo

The inhibitory action of SNPs was determined using a technique developed by Hajian-Maleki et al. [38] to determine therapeutic activity. The crops' roots and fruit were disinfected and inoculated with bacteria as per the following procedure. Each wound was inoculated with 30 µL of *Pcc* suspensions (about 1×10^8 CFU/mL). Six hours later, the SNP treatments' MIC was utilized. The control samples were inoculated with the pathogen, and were then treated with an equal amount of double-distilled water. The experiment was repeated three times with six tubers each time. All of the treatments were maintained in a humidified plastic packaging at room temperature. After a mild inoculation, just the longitudinal axis and the area across the inoculation site were sliced to quantify decay diameter (mm) and depth in SNP-treated and control tubers and fruit (d, mm). The disease rate was computed using the following equations: penetration (P, mm) based on rot depth and diameter, and reduction in incidence (percent RDI) based on lesion diameter: (2) P = [(D/2) + (d − 6)]/2 [39]. (3) % RDI = (D Positive control − D SNPs treatment)/D Positive control [40].

2.11. Statistical Analysis

Recorded data were subjected to analysis with SAS software (SAS Institute, version 9, Cary, NC, USA). Differences of $p \leq 0.05$ were regarded as significant and the means were separated using Duncan's multiple-range test.

3. Results

3.1. Visual Observation and UV-Vis Spectroscopy Studies

The fruit exudates of cork oak were exploited as a natural plant-based resource for green SNP synthetization in this study. During exposure to the exudates, the silver nitrate ions were reduced to SNPs, and after three distinct reaction periods (30, 60, and 120 min), a bright-brown color appeared, indicating the creation of SNPs (Figure 2). The SNPs' absorbance criteria are peaks between 400 and 450 nm.

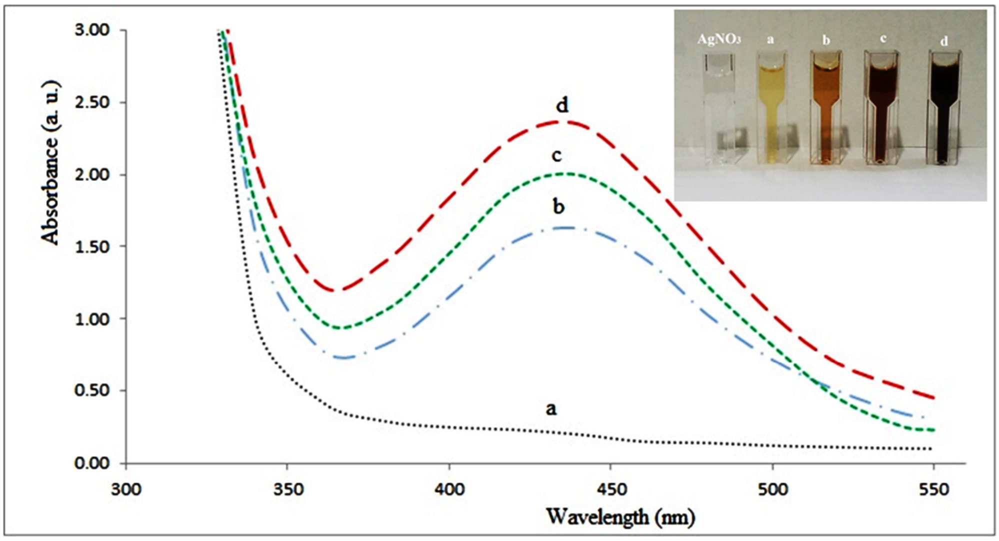

Figure 2. The UV-vis spectra and the exudate color change of biosynthesized silver nanoparticles (SNPs) at multiple-times exposure to $AgNO_3$, (**b**–**d**) are exudate, 30, 60 and 120 min after synthesis reaction, respectively and (**a**) is control (exudate solely).

3.2. Analysis of High-Resolution Transmission Electron Microscopy (TEM) and Atomic Force Microscopy (AFM)

The results of an electro-micrograph of SNPs demonstrated that the SNP formation is spherical, hexagonal, and amorphous. Figure 3 represents a TEM electro-micrograph of the biosynthesized SNPs of oak fruit exudates.

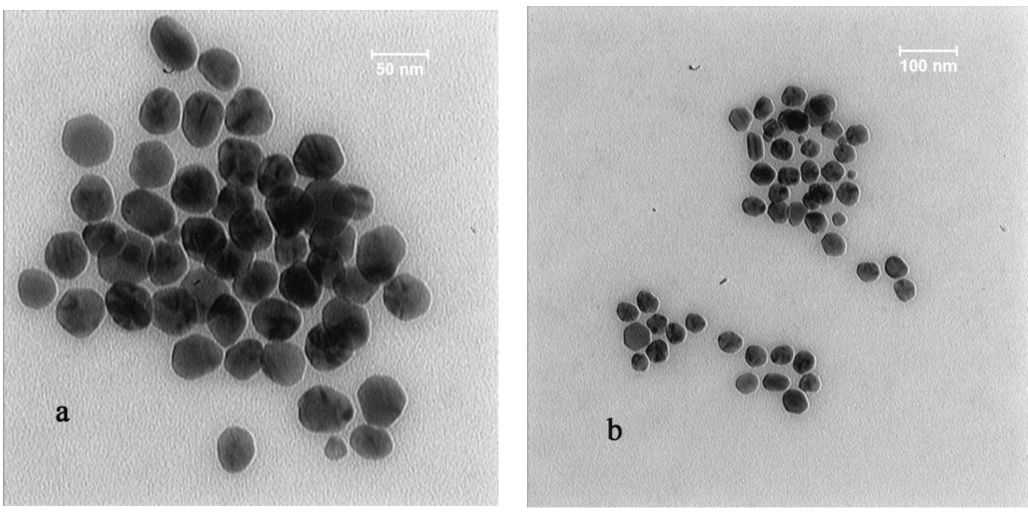

Figure 3. TEM studies of spherical silver nanoparticles ((**a**,**b**) different scales), synthesized (silver nanoparticles) in oak exudates.

Surfaces of generated SNPs studied by AFM are shown in one-dimensional (1D) and three-dimensional (3D) pictures, respectively. The AFM pictures indicate a distinct presence of spherical SNPs with varying particle sizes, as seen in Figure 4a,b.

3.3. XRD Analysis

The findings of X-ray diffraction (XRD) patterns indicate four sharp peaks in the whole spectrum of two theta values, ranging from 30 to 80, Figure 5. For the crystalline nature of the silver nanoparticles (SNPs), XRD peaks were seen about to be (111), (200), (220), and (311) planes at angles of 38, 44, 64, and 77°, respectively.

3.4. Dynamic Light Scattering (DLS) Analysis

The particle size was determined using the DLS method, and it was found to be 26.58 nm, 47.08 nm, and 80.07 nm in terms of number, volume, and intensity, respectively, with a polydispersity index (PDI) of 0.203 and a Z-average of 70.92 nm. The DLS histograms of the suspension of SNPs generated using oak fruit exudates are shown in Figure 6a–c. The SNPs were synthesized with a uniform distribution, which was validated. The zeta potential of the SNPs suspension is shown in Figure 6d.

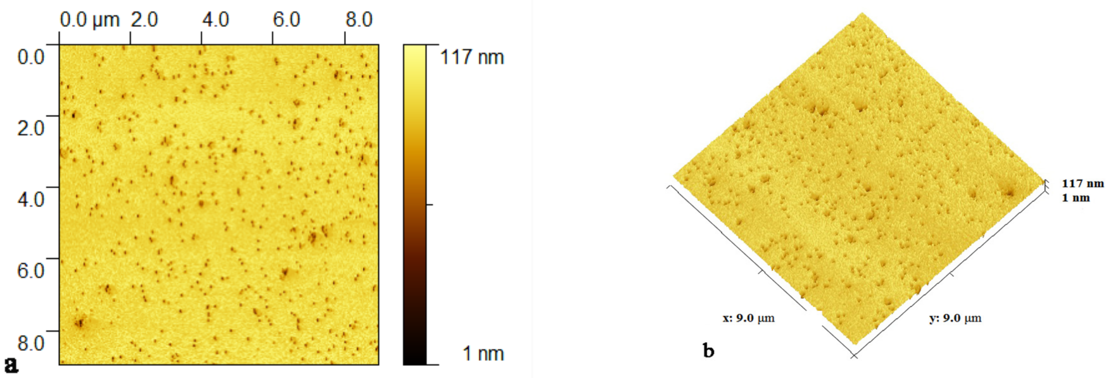

Figure 4. Atomic force microscopy (AFM) image analysis of silver nanoparticles (SNPs) green synthesized by oak exudates, indicative of typical presence of spherical SNPs, (**a**) 1D and (**b**) 3D.

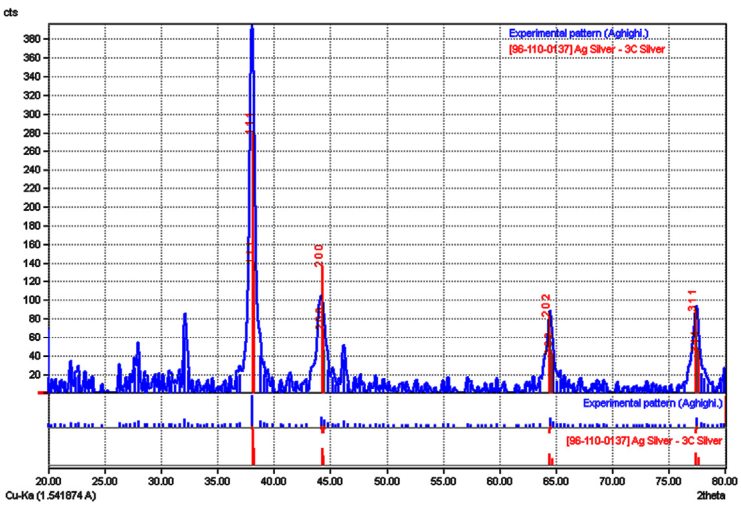

Figure 5. XRD analysis of silver nanoparticles biosynthesized by oak exudates shows four sharp peaks, indicating the crystalline nature of the biological synthesis SNPs.

3.5. FTIR Analysis

The interactions between molecules and the generated silver nanoparticles were studied using FTIR spectra. FTIR findings of synthesized SNPs are shown in Figure 7, which reveal several significant absorption peaks at 3365.92, 2925.31, 1732.64, 1450.17, and 1384.79 cm^{-1}. The amide bond of proteins from carbonyl stretching in natural proteins and aliphatic amines band may be ascribed to the absorption peak at 1615 cm^{-1} [30]. The O–H stretching associated with the O–H bond of H_2O molecules and carbohydrates is ascribed to the peak at 3365 cm^{-1} [41]. Furthermore, the absorption peak at 1628 cm^{-1} is similar to that of natural proteins, suggesting that proteins interact with manufactured SNPs [42]. The carboxyl, hydroxyl, and N–H groups in the oak fruit exudate are mostly involved in the conversion of Ag^{2+} ions to Ag^0 NPs, according to the FTIR data. The carboxyl, hydroxyl, and (N–H) groups in oak fruit exudates are most likely involved in the reduction of Ag^{2+} ions to Ag^0 NP, according to the FTIR study [43].

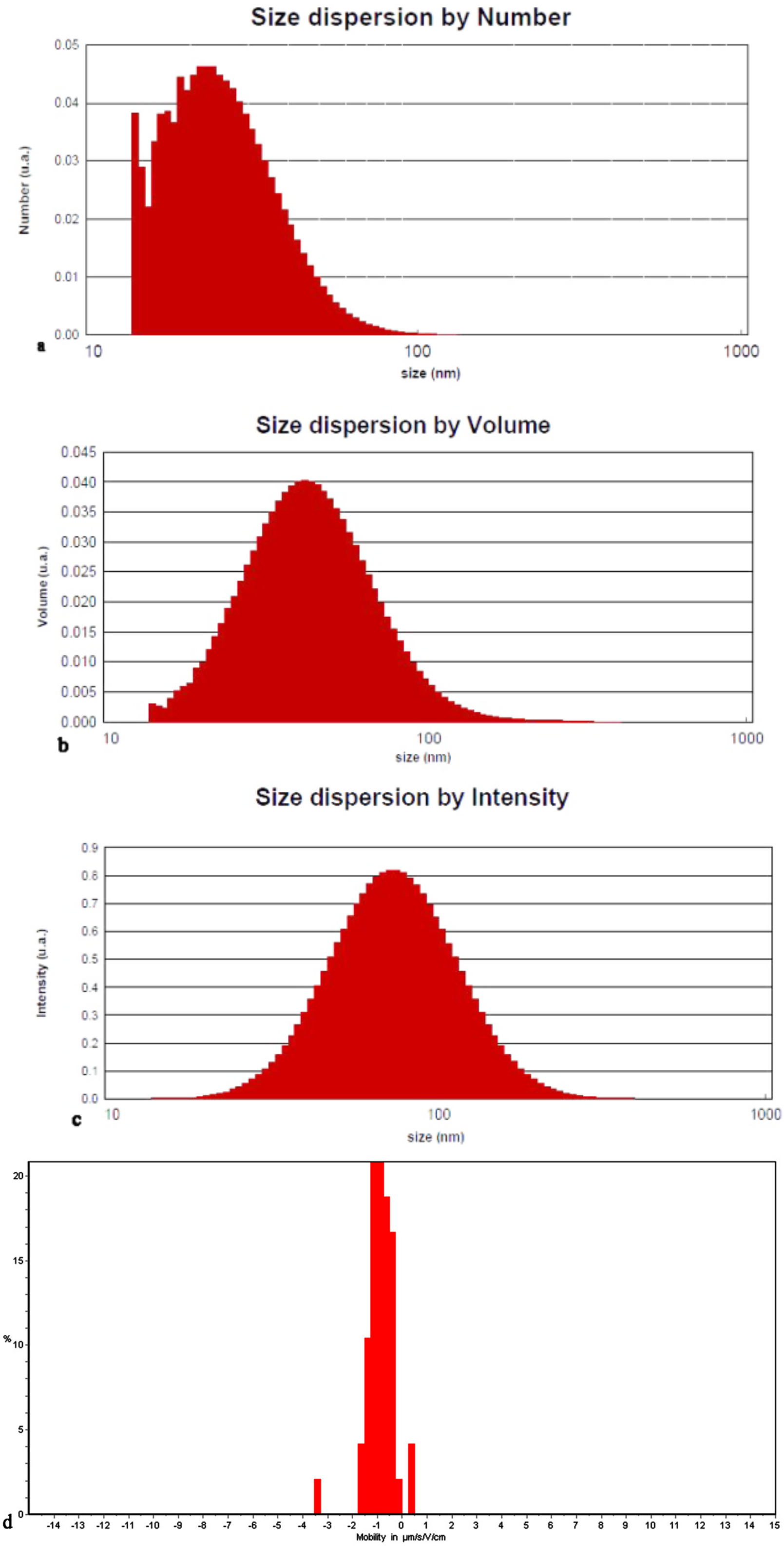

Figure 6. Dynamic light-scattering (DLS) micrographs that indicate size dispersion. (**a**) Number (26.58 nm), (**b**) volume (47.08), and (**c**) intensity (80.07); PDI is 0.203 and the other distributions at lower and higher ranges than nanoparticle size show that the synthesized particles are lower and higher in range in particle size and the uniform distribution of silver nanoparticles. (**d**) Indicate zeta potential measurement of the silver nanoparticle (SNP) suspension. Mobility mean 0.86 µm/s/V/cm; standard deviation: 0.57; zeta mean: −11.40 mV; standard deviation: 7.59.

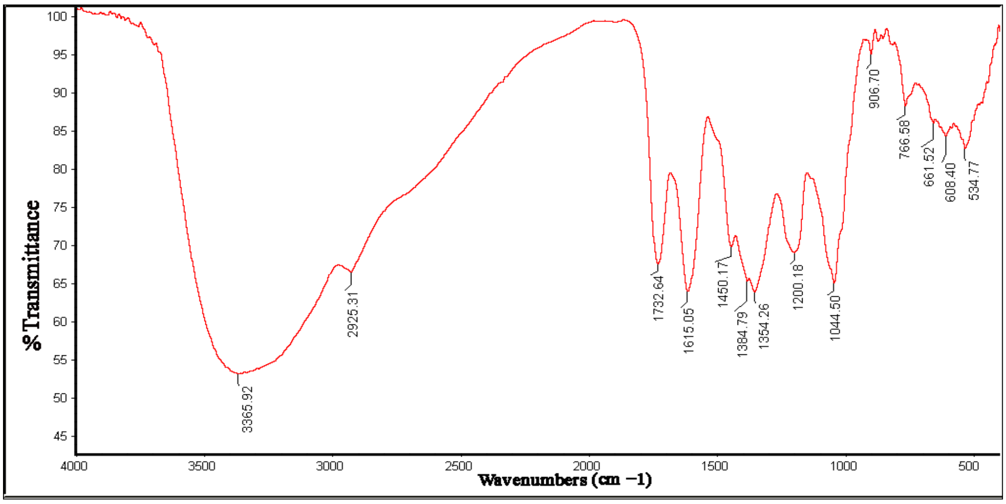

Figure 7. Fourier transform infrared spectroscopy (FTIR) spectrum of the phytosynthesized silver nanoparticles (SNPs) mediated by oak fruit exudates.

3.6. Antibacterial Activity of SNPs

We examined the antibacterial activity of silver nanoparticles mediated by oak fruit exudate as potential antibacterial agents against *Pcc* (strain 84). The existence of a growth inhibition zone surrounding the discs indicates antibacterial potential against the tested bacterium (Figure 8). Antibacterial characteristics were not found in the control group (just exudates). Streptomycin is a standard control antibiotic for a variety of phytopathogens, including *Pcc*, which was employed in all of the studies. The inhibitory zones surrounding the discs treated with SNPs were 8 ± 0.55 mm in diameter, compared to 14 ± 0.85 mm for the discs treated with streptomycin.

3.7. Evaluation of SNPs Effects on Pcc Growth

The in vitro growth index of *Pcc* in the presence of treated chemicals was examined in order to demonstrate that test materials had no growth inhibitory effects at certain levels. The growth of the pathogen was monitored until they reached the stationary phase. In the growth curve investigations, significant variations in the growth patterns of control and SNPs at tested doses were identified (Figure 9).

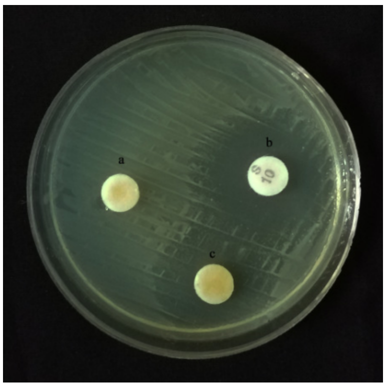

Figure 8. Antibacterial activity of photosynthesized SNPs against *Pcc* by the disk diffusion method: (**a**) control, (**b**) streptomycin, and (**c**) SNPs.

3.8. MIC and MBC Studies

The minimum inhibitory concentration (MIC µg/mL medium) and minimum bactericidal concentration (MBC, µg/mL medium) of the SNPs were identified as 150 and 200 µg/mL, respectively, Table 1.

Table 1. In vitro condition inhibitory effects of the SNPs against *Pcc*. The MIC and MBC were measured at 150 and 200 µg/mL, respectively. Control was oak exudate.

Growth (OD = 600 nm) / Concentration (µg/mL)	Treatments		
	Control	SNPs	Streptomycin
200	1.69 *a	0 b	0 b
150	1.72 a	0.05 b	0 b
100	1.75 a	0.11 bc	0 b
50	1.73 a	0.18 c	0 b
25	1.63 a	0.21 c	0 b
12.50	1.74 a	0.37 c	0 b
6.25	1.68 a	0.53 c	0.08 cb
3.12	1.77 a	0.92 ac	0.28 c
1.62	1.77 a	1.04 a	0.55 c
SE	0.58	0.05	0.03

* The presented analysis are the means of tree replications, and they are subjected to the analysis with the variance $n = 3$. For each trait, different letters indicate significant differences at $p \leq 0.05$ according to Duncan's Multiple Range Test.

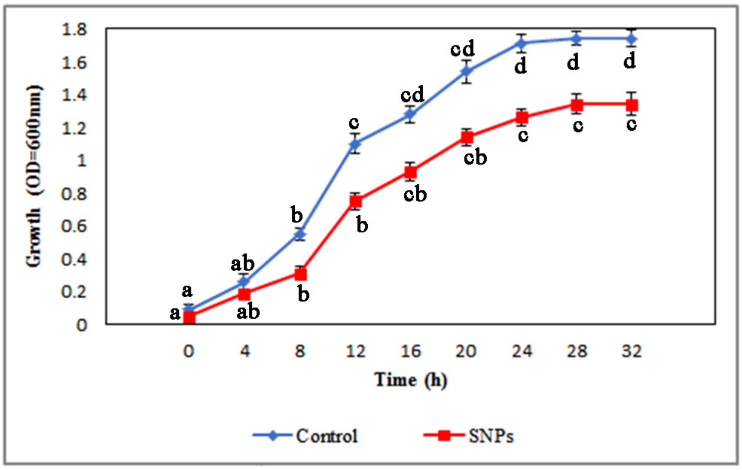

Figure 9. The growth curves of *Pectobacterium carotovorum* subsp. *crotovorum* (*Pcc*) in the presence of silver nanoparticles (SNPs) throughout a 32 h period, compared to control (without SNP addition). *Pcc* cells were exposed to sub-MIC SNPs in LB medium (different lowercase letters error bars represent standard error of the mean and Duncan's multiple range test, $p \leq 0.05$).

3.9. Inhibitory Effects of the SNPs on Soft Rot Disease in Tested Vegetables

When compared to the positive control (vegetables inoculated with bacteria), which exhibited the highest percentage of deterioration, the SNPs reduced soft rot symptoms on the individual fruits of zucchini and eggplant, potato tubers, and carrots (22, 19.8, 21.5, and 18.5 percent for potato (scale bar = 3 cm), zucchini, carrot, and eggplant, respectively). SNPs reduced the quantity of soft rot in potatoes by 12.6 and 13.5 percent, and 10.2 and 6.5 percent, respectively, in zucchini (scale bar = 25 cm), carrot (scale bar = 23 cm), and eggplant (scale bar = 15 cm), (Figure 10a,b).

3.10. In Vivo Curative Activity of SNPs against Soft Rot Disease

The in vivo test was used to assess the SNPs' curative effects at minimum inhibitory concentration (MIC) levels in order to identify a suitable control for soft rot disease in vivo (results are demonstrated in Table 2). The soft rot disease was dramatically reduced when the SNPs were used, according to our findings. When inoculation was conducted after the SNPs were applied, the infection incidence was reduced by 74.3, 57.2, 48.7, and 65.1 percent for potato, zucchini, carrot, and eggplant, respectively. In addition, as compared to controls, the vegetables treated with SNPs had a considerable reduction in soft rot penetration.

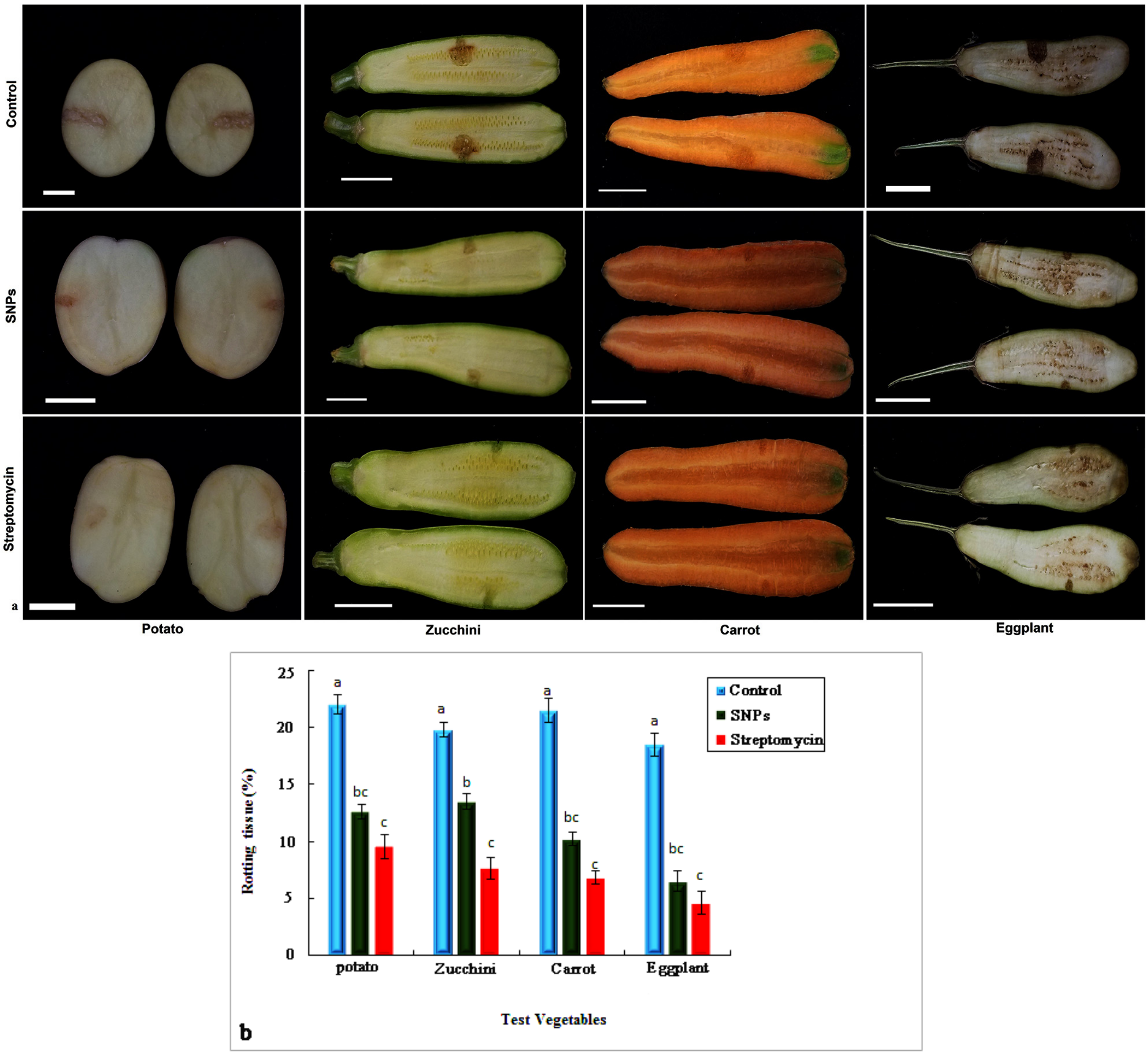

Figure 10. (**a**) In vitro examination of silver nanoparticles' (SNPs') inhibitory effects on vegetables against *Pectobacterium carotovorum* subsp *carotovorum* (*Pcc*), which causes soft rot. Soft rot symptoms were significantly reduced in SNP-treated tubers and fruits, compared to controls. As a positive control, streptomycin, was used. (**b**) The experiment was carried out three times. The standard error of the means is represented by error bars (three replicates). At $p \leq 0.05$, different letters indicate a significant difference.

Table 2. The effects of silver nanoparticles (SNPs) on soft rot in vegetables infected with pathogen. (30 µL of 1×10^8 CFU/mL) in in vivo conditions. The therapies were evaluated after a week, and the disease incidence and penetration were assessed. The experiment was repeated three times with three different replications each time. Significant differences are shown by different findings.

Treatments	SNPs		Control	
	RDI (%) a	P b	RDI (%)	P
Potato	74.3 ± 8.1	1.6 ± 0.4 ^{*b}	-	7.1 ± 0.5 ^{a}
Zucchini	57.2 ± 6.3	3.1 ± 0.3 ^{bc}	-	5.2 ± 0.3 ^{a}
Carrot	48.7 ± 5.7	3.4 ± 0.5 ^{bc}	-	4.9 ± 0.2 ^{a}
Eggplant	65.1 ± 5.9	2.8 ± 0.7 ^{b}	-	6.2 ± 0.6 ^{a}

RDI a—reduction of disease incidence. P b—penetration of soft rot disease in treated subjects (mm). * The labels a, b and c, when followed by another letter within the same column, indicate that the indicated values differ significantly ($p \leq 0.05$) according to Duncan's Multiple Range Test.

4. Discussion

Biosynthesis of SNPs from plant materials has fascinated scientists in the last decade, being a novel technique with a simple one-step methodology that does not produce hazardous chemicals. As a result, this method is very cost-effective, as well as ecologically benign and leaves minimally hazardous residues in soil and water [44–46]. The stronger the bactericidal activity, the bigger the surface area of the bacterial membrane, resulting in smaller SNPs, according to one probable mechanism for silver nanoparticles' antibacterial capabilities. The method through which SNPs affect pathogenic bacteria is as yet unknown. However, there are a few theories that explain why SNPs are antibacterial: (A) the release of Ag^+ ions from SNPs denaturizes proteins by interacting with sulfhydryl groups; (B) the adhesion of SNPs to bacteria and the subsequent damage to bacteria's capacity to live; (C) the attachment of SNPs to bacteria and the subsequent damage to bacteria's ability to survive (this results in high Ag^+ concentrations near the bacterial cell wall over time, inhibiting bacterial growth). However, a recent study has found that Ag^+ generated by SNPs may be antibacterial, resulting in cell damage or repercussions [47,48]. Positive silver ions interact with the negative cell membrane, causing morphological damage to the cell and subsequent cell leakage, which leads to cell death [49]. To boost bactericidal action, SNPs produce hydroxyl radicals. The cysteine moiety of proteins that interact with respiratory proteins has a strong affinity for silver ions with thiol groups [50]. SNPs with a high surface-to-volume ratio have a high capacity to interact with the cell layer by disturbing cell division structures and altering DNA and proteins in the same way that chain-affecting microorganisms' respiration and cell division. Increased levels of reactive oxygen species (ROS) in bacterial cells cause the transcription of genes that protect cells against ROS. A reactive oxygen species (ROS) is a kind of oxygen that is created during normal metabolism. To deal with this undesired chemical and avoid harm to important biomolecules inside the cell, universal intracellular defense systems have emerged. ROS levels may rise dramatically under intense stress, and their generation is thought to be one of the key NP modes of action that limits bacterial growth [51–53]. Silver nanoparticle characterizations were investigated using UV-vis spectroscopy, TEM, XRD, and FTIR. The intensity of color change from yellow to deep brown is directly related to the quantity of the oak exudate and the incubation period. This might be as the cause of the stimulation of longitudinal plasmon vibrations and $AgNO_3$ reduction [4]. In addition, the inhibitory activities of green synthesized AgNPs in sub-MIC concentration were investigated against *Pcc* as postharvest diseases. The FTIR spectra analysis revealed various absorption bands ranging from 530 to $4000\,cm^{-1}$. Such results represent the existence of potential biomolecules which probably mediate the reduction and stabilization of silver ions to silver nanoparticles available in aqueous fruit exudates [30]. We investigated the anti-pathogenic action of SNPs in our tests to support the results of the virulence trait experiments. In comparison to the control, the SNPs dramatically reduced the capacity of *Pcc* to cause infection. Our findings show that experimental SNPs could be used to prevent tissue rot and degeneration after infection. However, infection progression was seen to be greater with curative SNP therapy than during preventative application. The explanation for this might be that the microorganism has a 48 h window to permeate tissue under curative settings, and test chemicals are less likely to prevent infection transmission. This highlights the challenges we encounter when managing a disease after it has effectively penetrated plant tissue [38]. This study has generated useful information on the characterization of synthesized SNPs, utilizing cork oak fruit exudates (*Quercus brantii* L.). Furthermore, the antimicrobial effects of SNPs were shown in vitro and in vivo conditions. Accordingly, the antibacterial effects of the SNPs were dependent on their size, shape, and applied dosage. With all treatments, the disease incidence (percentage) of *Pcc* soft rot was dramatically reduced [54]. The smaller the silver nanoparticles were, the more silver ions they produced, posing a threat to the bacteria's function [55]. The cell walls of Gram-positive and Gram-negative bacteria are both negatively charged. This is a characteristic that is hypothesized to influence the interaction between the bacterial cell wall and the nanoparticles or ions generated by the bacterium [56]. According to the MIC and MBC tests, the SNPs' antibacterial activities against *Pcc* are less than streptomycin. Further research on the efficacy of bio-SNPs against different plant-pathogenic bacteria is suggested. Researchers should note that nanomaterials applied as food additives or as an antimicrobial agent have the most significant negative properties on human health, to an alarming extent [57].

The application of SNPs had a detrimental effect on the percentage of rotten tissue (RT percent), according to our findings. The information offered here might be applied as a foundation for future research with the goal of commercializing these SNP biosynthesized goods and moving toward sustainable agriculture. This method, we think, can be used to successfully manage comparable postharvest plant diseases. Furthermore, our study has produced information on the early phases of creating SNPs to protect crops from soft rot disease caused by *Pcc*. However, we insist that all bio-safety and health concerns of biosynthesized materials be examined in subsequent investigations before any large-scale production occurs.

5. Conclusions

We effectively employed oak fruit exudates for the green synthesis of silver nanoparticles, which led to the development of a new nano-pesticide. Plant-based biosynthesis is a fast, simple, safe, cost-effective, and more convenient process than chemical biosynthesis. SNPs had antibacterial effects that were proportional to their size and dosage. Further research on the efficacy of bio-SNPs against various postharvest plant diseases is suggested. Nanotechnology's potential advantages in postharvest disease control are widely known, and it has been shown to be the most promising tool in the development of novel antibacterial agents for bacterial infection management. Finally, based on our literature review, there is no record of fruit exudates of cork oak (*Quercus brantii* L.) being utilized to biosynthesize silver nanoparticles and being applied as a countermeasure against *Pcc* as a postharvest plant pathogen.

Author Contributions: All authors contributed different sections to this research article. Data collection, M.S.N.; formal analysis, N.S.N. and M.S.N.; methodology, M.S.N. and G.K.; project administration, M.S.N. and S.A.; supervision, S.A. and M.Z.; validation, S.A. and M.Z.; writing—original draft, M.S.N., N.S.N. and G.S.; writing—review and editing, S.A., A.B. and N.S.N. All authors have read and agreed to the published version of the manuscript.

Funding: This research received no external funding.

Data Availability Statement: Not applicable.

Acknowledgments: This paper is dedicated to the late A. Afzalipour and the late F. Saba, the founders of University of Kerman. The authors are thankful to Shahid Bahonar University of Kerman for providing the research facilities. This work was also supported by the RUDN University Strategic Academic Leadership program.

Conflicts of Interest: The authors declare no conflict of interest.

References

1. Bayda, S.; Adeel, M.; Tuccinardi, T.; Cordani, M.; Rizzolio, F. The history of nanoscience and nanotechnology: From chemical-physical applications to nanomedicine. *Molecules* **2019**, *25*, 112. [CrossRef]
2. Soltani Nejad, M.; Samandari Najafabadi, N.; Aghighi, S.; Pakina, E.; Zargar, M. Evaluation of *Phoma* sp. biomass as an endophytic fungus for synthesis of extracellular gold nanoparticles with antibacterial and antifungal properties. *Molecules* **2022**, *27*, 1181. [CrossRef]
3. Tarighi, S.; Soltani Nejad, M. Ecofriendly fabrication of silver nanoparticles using quince petal extract and its antibacterial properties against fire blight disease. *J. Nat. Pes. Res.* **2023**, *4*, 100026. [CrossRef]
4. Kumar, V.; Singh, S.; Srivastava, B.; Bhadouria, R.; Singh, R. Green synthesis of silver nanoparticles using leaf extract of *Holoptelea integrifolia* and preliminary investigation of its antioxidant, anti-inflammatory, antidiabetic and antibacterial activities. *J. Environ. Chem. Eng.* **2019**, *7*, 103094. [CrossRef]
5. Acidereli, H.; Karataş, Y.; Burhan, H.; Gülcan, M.; Şen, F. Chapter 8—Magnetic nanoparticles. In *Nanoscale Processing*; Thomas, S., Balakrishnan, P., Eds.; Elsevier: Amsterdam, The Netherlands, 2021; pp. 197–236.

6. Jorge de Souza, T.A.; Rosa Souza, L.R.; Franchi, L.P. Silver nanoparticles: An integrated view of green synthesis methods, transformation in the environment, and toxicity. *Ecotoxicol. Environ. Saf.* **2019**, *171*, 691–700. [CrossRef]
7. Soltani Nejad, M.; Bonjar, G.H.S.; Khatami, M.; Amini, A.; Aghighi, S. In vitro and in vivo antifungal properties of silver nanoparticles against *Rhizoctonia solani*, a common agent of rice sheath blight disease. *IET Nanobiotechnol.* **2017**, *11*, 236–240. [CrossRef]
8. Stater, E.P.; Sonay, A.Y.; Hart, C.; Grimm, J. The ancillary effects of nanoparticles and their implications for nanomedicine. *Nat. Nanotechnol.* **2021**, *16*, 1180–1194. [CrossRef]
9. Cho, I.-H.; Kim, D.H.; Park, S. Electrochemical biosensors: Perspective on functional nanomaterials for on-site analysis. *Biomater. Res.* **2020**, *24*, 6. [CrossRef]
10. Zhou, Y.-H.; Mujumdar, A.S.; Vidyarthi, S.K.; Zielinska, M.; Liu, H.; Deng, L.-Z.; Xiao, H.-W. Nanotechnology for food safety and security: A Comprehensive Review. *Food Rev. Int.* **2021**, 1–21. [CrossRef]
11. Neme, K.; Nafady, A.; Uddin, S.; Tola, Y.B. Application of nanotechnology in agriculture, postharvest loss reduction and food processing: Food security implication and challenges. *Heliyon* **2021**, *7*, e08539. [CrossRef]
12. Mittal, D.; Kaur, G.; Singh, P.; Yadav, K.; Ali, S.A. Nanoparticle-based sustainable agriculture and food science: Recent advances and future outlook. *Front. Nanotechnol.* **2020**, *2*, 10. [CrossRef]
13. Patil, S.; Chandrasekaran, R. Biogenic nanoparticles: A comprehensive perspective in synthesis, characterization, application and its challenges. *J. Genet. Eng. Biotechnol.* **2020**, *18*, 67. [CrossRef] [PubMed]
14. Ying, S.; Guan, Z.; Ofoegbu, P.C.; Clubb, P.; Rico, C.; He, F.; Hong, J. Green synthesis of nanoparticles: Current developments and limitations. *Environ. Technol. Innov.* **2022**, *26*, 102336. [CrossRef]
15. Rane, A.V.; Kanny, K.; Abitha, V.K.; Thomas, S. Chapter 5—Methods for Synthesis of Nanoparticles and Fabrication of Nanocomposites. In *Synthesis of Inorganic Nanomaterials*; Mohan Bhagyaraj, S., Oluwafemi, O.S., Kalarikkal, N., Thomas, S., Eds.; Woodhead Publishing: Cambridge, UK, 2018; pp. 121–139.
16. Jain, S.; Mehata, M.S. Medicinal plant leaf extract and pure flavonoid mediated green synthesis of silver nanoparticles and their enhanced antibacterial property. *Sci. Rep.* **2017**, *7*, 15867. [CrossRef]
17. Hasan, K.M.F.; Xiaoyi, L.; Shaoqin, Z.; Horváth, P.G.; Bak, M.; Bejó, L.; Sipos, G.; Alpár, T. Functional silver nanoparticles synthesis from sustainable point of view: 2000 to 2023—A review on game changing materials. *Heliyon* **2022**, *8*, e12322. [CrossRef]
18. Narayanan, M.; Divya, S.; Natarajan, D.; Senthil-Nathan, S.; Kandasamy, S.; Chinnathambi, A.; Alahmadi, T.A.; Pugazhendhi, A. Green synthesis of silver nanoparticles from aqueous extract of *Ctenolepis garcini* L. and assess their possible biological applications. *Process Biochem.* **2021**, *107*, 91–99. [CrossRef]
19. Jalab, J.; Abdelwahed, W.; Kitaz, A.; Al-Kayali, R. Green synthesis of silver nanoparticles using aqueous extract of *Acacia cyanophylla* and its antibacterial activity. *Heliyon* **2021**, *7*, e08033. [CrossRef]
20. Yang, B.; Gao, Y.; Zhang, C.; Han, J.; Liu, Y.; Zheng, X. Potato (*Solanum tuberosum* L.) can be grown safety on human consumption in slight Hg-contaminated soils across China mainland. *Sci. Rep.* **2020**, *10*, 8351. [CrossRef]
21. Czajkowski, R.; Pérombelon, M.C.M.; Jafra, S.; Lojkowska, E.; Potrykus, M.; van der Wolf, J.M.; Sledz, W. Detection, identification and differentiation of *Pectobacterium* and *Dickeya* species causing potato blackleg and tuber soft rot: A review. *Ann. Appl. Biol.* **2015**, *166*, 18–38. [CrossRef]
22. Abd-El-Khair, H.; Abdel-Gaied, T.G.; Mikhail, M.S.; Abdel-Alim, A.I.; El-Nasr, H.I.S. Biological control of *Pectobacterium carotovorum* subsp. *carotovorum*, the causal agent of bacterial soft rot in vegetables, in vitro and in vivo tests. *Bull. Natl. Res. Cent.* **2021**, *45*, 37. [CrossRef]
23. Kang, M.; Kim, S.-J.; Lee, J.Y.; Yoon, S.-R.; Kim, S.H.; Ha, J.-H. Inactivation of *Pectobacterium carotovorum* subsp. *carotovorum* on Chinese cabbage (*Brassica rapa* L. subsp. *pekinensis*) by wash treatments with phenolic compounds. *LWT* **2018**, *93*, 229–236. [CrossRef]
24. Bayat, M.; Kavhiza, N.; Orujov, E.; Zargar, M.; Akhrarov, M.; Temewei, A.G. Integrated weed control methods utilizing planting pattern in sugar beet. *Res. Crops* **2019**, *20*, 413–418.
25. Nouri, M.; Baghaee-Ravari, S.; Emadzadeh, B. Nano-emulsified savory and thyme formulation show limited efficacy to suppress *Pectobacterium carotovorum* subsp. *carotovorum* compared with pure oil. *Ind. Crops Prod.* **2021**, *161*, 113216. [CrossRef]
26. Yi, L.; Liu, X.; Qi, T.; Deng, L.; Zeng, K. A new way to reduce postharvest loss of vegetables: Antibacterial products of vegetable fermentation and its controlling soft rot caused by *Pectobacterium carotovorum*. *Biol. Control* **2021**, *161*, 104708. [CrossRef]
27. Choi, O.; Kim, J. *Pectobacterium carotovorum* subsp. *brasiliense* Causing Soft Rot on Paprika in Korea. *J. Phytopathol.* **2013**, *161*, 125–127. [CrossRef]
28. Siddiqui, Z.A.; Hashmi, A.; Khan, M.R.; Parveen, A. Management of bacteria *Pectobacterium carotovorum*, *Xanthomonas campestris* pv. *carotae*, and fungi *Rhizoctonia solani*, *Fusarium solani* and *Alternaria dauci* with silicon dioxide nanoparticles on carrot. *J. Veg. Sci.* **2020**, *26*, 547–557. [CrossRef]
29. Catara, V.; Bella, P.; Polizzi, G.; Paratore, A. First report of bacterial stem rot caused by *Pectobacterium carotovorum* subsp. *carotovorum* and *P. carotovorum* subsp. *atrosepticum* on grafted eggplant in Italy. *Plant Dis.* **2001**, *85*, 921. [CrossRef]
30. Soltani Nejad, M.; Samandari Najafabadi, N.; Aghighi, S.; Shahidi Bonjar, A.H.; Murtazova, K.M.-S.; Nakhaev, M.R.; Zargar, M. Investigating the potential of *Streptomyces* spp. in suppression of *Rhizoctonia solani* (AG1-IA) causing rice sheath blight disease in northern Iran. *Agronomy* **2022**, *12*, 2292. [CrossRef]

31. García-Pastor, M.E.; Falagán, N.; Giné-Bordonaba, J.; Wójcik, D.A.; Terry, L.A.; Alamar, M.C. Cultivar and tissue-specific changes of abscisic acid, its catabolites and individual sugars during postharvest handling of flat peaches (*Prunus persica* cv. *platycarpa*). *Postharvest Biol. Technol.* **2021**, *181*, 111688. [CrossRef]
32. Lutz, M.C.; Colodner, A.; Tudela, M.A.; Carmona, M.A.; Sosa, M.C. Antifungal effects of low environmental risk compounds on development of pear postharvest diseases: Orchard and postharvest applications. *Sci. Hortic.* **2022**, *295*, 110862. [CrossRef]
33. Khatami, M.; Nejad, M.S.; Salari, S.; Almani, P.G.N. Plant-mediated green synthesis of silver nanoparticles using *Trifolium resupinatum* seed exudate and their antifungal efficacy on *Neofusicoccum parvum* and *Rhizoctonia solani*. *IET Nanobiotechnol.* **2016**, *10*, 237–243. [CrossRef] [PubMed]
34. Pirtarighat, S.; Ghannadnia, M.; Baghshahi, S. Green synthesis of silver nanoparticles using the plant extract of *Salvia spinosa* grown in vitro and their antibacterial activity assessment. *Chem. Chem.* **2019**, *9*, 1–9. [CrossRef]
35. Rautela, A.; Rani, J.; Debnath, M. Green synthesis of silver nanoparticles from *Tectona grandis* seeds extract: Characterization and mechanism of antimicrobial action on different microorganisms. *J. Anal. Sci. Technol.* **2019**, *10*, 5. [CrossRef]
36. Soltani Nejad, M.; Khatami, M.; Shahidi Bonjar, G.H. Extracellular synthesis gold nanotriangles using biomass of *Streptomyces microflavus*. *IET Nanobiotechnol.* **2016**, *10*, 33–38. [CrossRef] [PubMed]
37. Akhlaghi, M.; Tarighi, S.; Taheri, P. Effects of plant essential oils on growth and virulence factors of *Erwinia amylovora*. *J. Plant Pathol.* **2020**, *102*, 409–419. [CrossRef]
38. Hajian-Maleki, H.; Baghaee-Ravari, S.; Moghaddam, M. Efficiency of essential oils against *Pectobacterium carotovorum* subsp. *carotovorum* causing potato soft rot and their possible application as coatings in storage. *Postharvest Biol. Technol.* **2019**, *156*, 110928. [CrossRef]
39. Zargar, M.; Pakina, E. Reduced rates of herbicide combined with biological components for suppressing weeds in wheat fields of Moscow, Russia. *Res. Crops* **2014**, *15*, 332–338. [CrossRef]
40. Sameza, M.L.; Nguemnang Mabou, L.C.; Tchameni, S.N.; Boat Bedine, M.A.; Tchoumbougnang, F.; Jazet Dongmo, P.M.; Boyom Fekam, F. Evaluation of clove essential oil as a mycobiocide against *Rhizopus stolonifer* and *Fusarium solani*, tuber rot causing fungi in yam (*Dioscorea rotundata* Poir.). *J. Phytopathol.* **2016**, *164*, 433–440. [CrossRef]
41. Sabouri, Z.; Rangrazi, A.; Amiri, M.S.; Khatami, M.; Darroudi, M. Green synthesis of nickel oxide nanoparticles using *Salvia hispanica* L. (chia) seeds extract and studies of their photocatalytic activity and cytotoxicity effects. *Bioprocess Biosyst. Eng.* **2021**, *44*, 2407–2415. [CrossRef]
42. Sharma, P.; Pant, S.; Rai, S.; Yadav, R.B.; Dave, V. Green synthesis of silver nanoparticle capped with *Allium cepa* and their catalytic reduction of textile dyes: An ecofriendly approach. *J. Polym.* **2018**, *26*, 1795–1803. [CrossRef]
43. Soltani Nejad, M.; Khatami, M.; Shahidi Bonjar, G.H. *Streptomyces somaliensis* mediated green synthesis of silver nanoparticles. *Nanomed. J.* **2015**, *2*, 217–222. [CrossRef]
44. Askari, Z.; Vahabi, M.R.; Allafchian, A.; Mousavi, S.A.; Jalali, S.A.H. Biosynthesis of antibacterial silver nanoparticles using *Astragalus verus* Olivier. *Micro Nano Lett.* **2020**, *15*, 66–71. [CrossRef]
45. Stabryla, L.M.; Johnston, K.A.; Diemler, N.A.; Cooper, V.S.; Millstone, J.E.; Haig, S.-J.; Gilbertson, L.M. Role of bacterial motility in differential resistance mechanisms of silver nanoparticles and silver ions. *Nat. Nanotechnol.* **2021**, *16*, 996–1003. [CrossRef] [PubMed]
46. Urnukhsaikhan, E.; Bold, B.-E.; Gunbileg, A.; Sukhbaatar, N.; Mishig-Ochir, T. Antibacterial activity and characteristics of silver nanoparticles biosynthesized from *Carduus crispus*. *Sci. Rep.* **2021**, *11*, 21047. [CrossRef] [PubMed]
47. Tang, S.; Zheng, J. Antibacterial activity of silver nanoparticles: Structural effects. *Adv. Healthc. Mater.* **2018**, *7*, 1701503. [CrossRef]
48. Alizadeh, A.; Salouti, M.; Alizadeh, H.; Kazemizadeh, A.R.; Safari, A.A.; Mahmazi, S. Enhanced antibacterial effect of azlocillin in conjugation with silver nanoparticles against *Pseudomonas aeruginosa*. *IET Nanobiotechnol.* **2017**, *11*, 942–947. [CrossRef]
49. Zhang, C.; Hu, Z.; Deng, B. Silver nanoparticles in aquatic environments: Physiochemical behavior and antimicrobial mechanisms. *Water Res.* **2016**, *88*, 403–427. [CrossRef]
50. Kalwar, K.; Shan, D. Antimicrobial effect of silver nanoparticles (AgNPs) and their mechanism a mini review. *Micro Nano Lett.* **2018**, *13*, 277–280. [CrossRef]
51. Ivask, A.; ElBadawy, A.; Kaweeteerawat, C.; Boren, D.; Fischer, H.; Ji, Z.; Chang, C.H.; Liu, R.; Tolaymat, T.; Telesca, D. Toxicity mechanisms in *Escherichia coli* vary for silver nanoparticles and differ from ionic silver. *ACS Nano* **2014**, *8*, 374–386. [CrossRef]
52. Ghadamkheir, M.; Vladimirovich, K.P.; Orujov, E.; Bayat, M.; Madumarov, M.M.; Avdotyin, V.; Zargar, M. Influence of sulfur fertilization on infection of wheat Take-all disease caused by the fungus *Gaeumannomyces graminis* var. tritici. *Res. Crops* **2020**, *21*, 627–633.
53. Madl, A.K.; Plummer, L.E.; Carosino, C.; Pinkerton, K.E. Nanoparticles, lung injury, and the role of oxidant stress. *Annu. Rev. Plant Physiol.* **2014**, *76*, 447–465. [CrossRef] [PubMed]
54. Ghazy, N.A.; Abd El-Hafez, O.A.; El-Bakery, A.M.; El-Geddawy, D.I.H. Impact of silver nanoparticles and two biological treatments to control soft rot disease in sugar beet (*Beta vulgaris* L.). *Egypt. J. Biol. Pest Control* **2021**, *31*, 3. [CrossRef]
55. Tripathi, D.K.; Singh, S.; Singh, S.; Pandey, R.; Singh, V.P.; Sharma, N.C.; Prasad, S.M.; Dubey, N.K.; Chauhan, D.K. An overview on manufactured nanoparticles in plants: Uptake, translocation, accumulation and phytotoxicity. *Plant Physiol. Biochem.* **2017**, *110*, 2–12. [CrossRef] [PubMed]

56. Slavin, Y.N.; Asnis, J.; Häfeli, U.O.; Bach, H. Metal nanoparticles: Understanding the mechanisms behind antibacterial activity. *J. Nanobiotechnol.* **2017**, *15*, 65. [CrossRef]
57. Sahani, S.; Sharma, Y.C. Advancements in applications of nanotechnology in global food industry. *Food Chem.* **2021**, *342*, 128318. [CrossRef]

Disclaimer/Publisher's Note: The statements, opinions and data contained in all publications are solely those of the individual author(s) and contributor(s) and not of MDPI and/or the editor(s). MDPI and/or the editor(s) disclaim responsibility for any injury to people or property resulting from any ideas, methods, instructions or products referred to in the content.